

## Lattice instabilities near the critical V-V separation for localized versus itinerant electrons in $\text{LiV}_{1-y}\text{M}_y\text{O}_2$ ( $M = \text{Cr}$ or $\text{Ti}$ ) and $\text{Li}_{1-x}\text{VO}_2$

J. B. Goodenough, G. Dutta, and A. Manthiram

Center for Materials Science and Engineering, ETC 5. 160, University of Texas at Austin, Austin, Texas 78712-1084

(Received 15 November 1990)

From the compositional dependences of the lattice parameters in the system  $\text{LiV}_{1-y}\text{Cr}_y\text{O}_2$ , a critical V-V separation  $R_c = 2.90 \pm 0.01 \text{ \AA}$  has been determined for an array of octahedral-site  $\text{V}^{3+}$  ions sharing common octahedral-site edges with six like nearest neighbors. A first-order transition on passing from the itinerant-electron regime  $R < R_c$  to the localized-electron regime  $R > R_c$  was also established. In  $\text{LiVO}_2$ , the electron instability associated with an  $R \approx R_c$  is manifest by  $\text{V}_3$  trimer formation at temperatures  $T < 490 \text{ K}$  with  $R < R_c$  within a trimer and  $R > R_c$  between trimers. Introduction of a mixed valence in  $\text{Li}_{1-x}\text{VO}_2$  results in a two-phase mixture in the interval  $0 < x \lesssim 0.12$ ; the metastable  $\text{Li}_{1-x}\text{VO}_2$  phase in the interval  $0.12 \lesssim x \lesssim 0.33$  disproportionates above a  $T' \approx 550 \text{ K}$  into  $\text{LiVO}_2$  and  $\text{Li}[\text{V}_2]\text{O}_4$ . Comparisons are made between the instabilities associated with a  $W \approx U$  in the copper oxide superconductors and those in the layered and spinel vanadium oxides. In particular, attention is called to evidences for dynamic charge-density fluctuations that appear to be associated with superconductivity in the copper oxides, but not in the vanadium oxides.

### I. INTRODUCTION

$\text{LiVO}_2$  crystallizes in an ordered rocksalt structure with  $\text{Li}^+$  and  $\text{V}^{3+}$  ions occupying alternate (111) planes. Like the antiferromagnetic semiconductor  $\text{La}_2\text{CuO}_4$ , the compound  $\text{LiVO}_2$  has a half-filled, essentially two-dimensional (2D)  $3d$  band. In addition, the on-site correlation energies  $U$  are large enough to inhibit the formation of a negative- $U$  charge-density wave (CDW) in any known vanadium or copper oxide. In a negative- $U$  CDW, electrons are transferred from one subset of like cations to another as in  $\text{BaBiO}_3$  where  $2\text{Bi(IV)} \rightarrow \text{Bi}_I(\text{IV}-\delta) + \text{Bi}_{II}(\text{IV}+\delta)$ . On the other hand,  $\text{La}_2\text{CuO}_4$  has a bandwidth  $W$  arising from nearly  $180^\circ$  Cu-O-Cu interactions whereas  $\text{LiVO}_2$  has a bandwidth arising from V-V interactions across shared octahedral-site edges.

In the superconductor compositions  $\text{La}_2\text{CuO}_{4+\delta}$  and  $\text{La}_{2-x}\text{Sr}_x\text{CuO}_4$ , oxidation of the  $\text{CuO}_2$  sheets beyond  $(\text{CuO}_2)^{2-}$  creates a condition  $W \approx U$ , and it has been conjectured<sup>1</sup> that the origin of the high- $T_c$  superconductivity resides in strong electron-phonon interactions associated with lattice instabilities that inevitably arise where the condition  $W \approx U$  is present. Others<sup>2</sup> have also conjectured that there are inherent lattice instabilities in the superconductive copper oxides, but they attribute them to a Van Hove singularity at, or near, the Fermi energy. Of course, there have been many other speculations concerning the mechanism of high- $T_c$  superconductivity that ignore any role associated with lattice instabilities.<sup>3</sup> It is precisely for this reason that we focus attention here on the question of lattice instabilities in compounds with a bandwidth  $W \approx U$ .

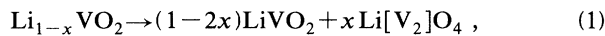
$\text{LiVO}_2$  exhibits a first-order structural transition with an order of magnitude increase in the magnetic susceptibility on increasing the temperature through  $T_i \approx 490 \text{ K}$

(Ref. 3); this transition has been interpreted<sup>4</sup> to be due to formation of a CDW created by a clustering of the V atoms within a V plane into  $\text{V}_3$  trimers, and Bongers<sup>5</sup> has provided experimental evidence to support this interpretation. In this paper we argue that the V-V separation within a basal plane of  $\text{LiVO}_2$  is  $R \approx R_c$ , where  $R_c$  is a critical separation corresponding to a  $W \approx U$ . In  $\text{LiVO}_2$  and  $\text{Li}_{1-x}\text{VO}_2$ , the lattice displacements that express the instability inherent in a  $W \approx U$ , i.e.,  $R \approx R_c$ , are static whereas in the copper oxide superconductors they are postulated to be dynamic. Whether this difference is due to metal-metal interactions in the one case and metal-oxygen-metal interactions in the other remains an open question. However, recent magnetic-susceptibility<sup>6</sup> and NMR data<sup>7</sup> on the spinel system  $\text{Li}_x\text{Zn}_{1-x}[\text{V}_2]\text{O}_4$  indicate that the  $\text{V}^{3+}$  ions in  $\text{Zn}[\text{V}_2]\text{O}_4$  and Zn-rich regions of  $\text{Li}_x\text{Zn}_{1-x}[\text{V}_2]\text{O}_4$  may exhibit below  $500 \text{ K}$  a dynamic V-V clustering with  $R \rightarrow R_c$ . What we are interested in establishing is the appearance of inherent lattice instabilities associated with a  $W \approx U$ ; we believe these are significant whether they find expression in a static CDW or in dynamic fluctuations with/without superconductivity. If lattice instabilities are an intrinsic aspect of a system with  $W \approx U$ , then it is not necessary to invoke a Van Hove singularity to account for the high- $T_c$  superconductivity found in the copper oxides with  $W \approx U$ .

We report here an investigation of the systems  $\text{LiV}_{1-y}\text{Cr}_y\text{O}_2$  and  $\text{LiV}_{1-y}\text{Ti}_y\text{O}_2$  to determine a critical V-V separation  $R_c$  for the transition from strongly ( $R > R_c, W < U$ ) to weakly ( $R < R_c, W > U$ ) correlated electrons in a V  $3d$  band associated with octahedral-site  $\text{V}^{3+}$  ions sharing common octahedral-site edges with six like nearest neighbors in an oxide. Moreover, we demonstrate that the transition is not smooth, but first-order, in support of the contention that lattice instabilities are implicit in any system where  $R \approx R_c$ , i.e.,  $W \approx U$ . We also

distinguish the value of  $R_c$  obtained for a single-valent system from the value of  $R$  at which the transport properties change, in a mixed-valent system, from small-polaron behavior with a motional enthalpy  $\Delta H_m > 0$  to transport where  $\Delta H_m = 0$ . However, identification of the latter may be complicated by the formation of distinguishable electronic pathways in a system made mixed-valent by doping.

In addition, we demonstrate the existence of a distinguishable low-temperature phase with a different transition temperature  $T'_i$  in the system  $\text{Li}_{1-x}\text{VO}_2$  obtained by room-temperature extraction of Li from  $\text{LiVO}_2$ . The transition in  $\text{LiVO}_2$  is reversible on thermal cycling through  $T_i$ ; heating  $\text{Li}_{1-x}\text{VO}_2$  ( $0.12 \leq x \leq 0.33$ ) through its transition temperature  $T'_i \approx 550$  K results in the disproportionation reaction<sup>8</sup>



which is irreversible. We present the compositional dependences of  $T_i$  and  $T'_i$  and the enthalpy changes  $\Delta H$  on crossing  $T_i$  and  $T'_i$ ; we also argue that they support a model in which  $T_i$  and  $T'_i$  are determined by the change in lattice energy due to the structural change rather than by the enthalpy  $\Delta H$  of the transition.

## II. EXPERIMENTAL

The  $\text{LiV}_{1-y}\text{M}_y\text{O}_2$  ( $M = \text{Ti}$  or  $\text{Cr}$ ) samples were obtained by firing an intimate mixture of required quantities of  $\text{Li}_2\text{CO}_3$ ,  $\text{V}_2\text{O}_5$ , and  $\text{Cr}_2\text{O}_3$  or  $\text{TiO}$  and  $\text{TiO}_2$  under flowing  $\text{H}_2$  atm first at 770 K for 5 h to release  $\text{CO}_2$  and then at 970 K for 15 h. Although this firing schedule leads to single-phase material for  $y = 0$ , it also produces traces of impurity phases for  $y > 0$ . Therefore all products with  $y > 0$  were further fired in flowing  $\text{N}_2$  at 1020 K for 24 h for  $M = \text{Cr}$  and at 970 K for 15 h for  $M = \text{Ti}$ ; they were then quenched in  $\text{N}_2$  atm to ambient temperature. The additional heat treatment yielded single-phase samples for  $0 < y \leq 0.2$  with  $M = \text{Ti}$ . The end member  $\text{LiCrO}_2$  was prepared by firing required quantities of  $\text{Li}_2\text{CO}_3$  and  $\text{Cr}_2\text{O}_3$  under flowing  $\text{N}_2$  at 770 K for 5 h, 970 K for 15 h, and finally 1070 K for 24 h. Since commercial  $\text{Cr}_2\text{O}_3$  is too refractory, a "soft"  $\text{Cr}_2\text{O}_3$  was used. The soft  $\text{Cr}_2\text{O}_3$  was obtained by the precipitation of  $\text{Cr}_2\text{O}_3 \cdot x\text{H}_2\text{O}$  gel from  $\text{Cr}(\text{NO}_3)_3 \cdot \xi\text{H}_2\text{O}$  with  $\text{NH}_4\text{OH}$  and driving off the water from the gel at 600°C for 1 h.

The  $\text{Li}_{1-x}\text{VO}_2$  samples with  $0 \leq x \leq 0.33$  were obtained by extracting Li from  $\text{LiVO}_2$  at room temperature with a calculated amount of  $\text{Br}_2$  (0.05 N in chloroform solution).<sup>8,9</sup> Since oxidants absorbed on the surface of  $\text{LiVO}_2$  are known to extract Li from the bulk at ambient temperature,<sup>8</sup> exposure to air was avoided; the samples were stored in an argon-filled dry box immediately after preparation.

All samples were characterized by x-ray powder diffraction recorded with a Philips diffractometer and  $\text{Cu K}\alpha$  radiation. The Li content was determined by atomic absorption with a Perkin-Elmer 1100 atomic absorption spectrometer after calibrating the instrument with a lithium carbonate solution of known concentration.

Differential scanning calorimetry (DSC) plots were recorded in  $\text{N}_2$  atm at  $10^\circ\text{C min}^{-1}$  with a Perkin-Elmer Series 7 thermal analysis system.

## III. A CRITICAL V-V SEPARATION $R_c$

### A. Review of the problem

The  $\text{V}^{3+}$  ions of  $\text{LiVO}_2$  occupy octahedral sites sharing common octahedral-site edges with  $z = 6$  like near neighbors in a close-packed  $\text{V}^{3+}$ -ion plane. Each  $\text{V}^{3+}$  ion has two  $3d$  electrons; the trigonal crystalline field removes the  $t_2$ -orbital degeneracy to create an empty  $a_1$  orbital normal to the plane and twofold-degenerate  $e_\pi$  orbitals directed toward nearest-neighbor  $\text{V}^{3+}$  ions within a basal plane. Thus the crystal symmetry removes an orbital degeneracy to create a narrow, half-filled, two-dimensional (2D)  $3d$  band of  $e_\pi$  parentage. The band is twofold-degenerate, and the bandwidth—in tight-binding theory  $W \approx 2zb$ —varies exponentially with the V-V separation  $R$  via the matrix element

$$b \equiv (\psi_i, H' \psi_j) \approx \varepsilon (\psi_i, \psi_j), \quad (2)$$

where  $H'$  is the perturbation of the  $e_\pi$ -electron potential at  $\mathbf{R}_j$  due to the presence of a neighboring like atom at  $\mathbf{R}_i$ ,  $\varepsilon$  is a one-electron energy, and  $(\psi_i, \psi_j)$  is an overlap integral. A  $(\psi_i, \psi_j) \sim \exp(-R/\rho)$ , where  $\rho$  is a parameter of units of  $R$ , arises from the overlap integral for a V-V interaction across an interatomic distance  $R$ . At low temperature  $T < T_i$ , the formation of  $\text{V}_3$  trimers, Fig. 1, would change the translational symmetry so as to split the 2D half-filled V  $3d$  band in two; an  $R < R_c$  within a cluster and an  $R > R_c$  between clusters would result in the capture of conduction electrons within molecular orbitals. A change in translational rather than point-group symmetry is taken<sup>4</sup> to signal an  $R \lesssim R_c$  at temperatures  $T > T_i$ , and a more recent report<sup>10</sup> that strong infrared bands appearing below  $T_i$  disappear on crossing  $T_i$  supports this view. Bongers<sup>3</sup> reported that on increasing the temperature through  $T_i$ , the axial  $c/a$  ratio (hexagonal basis) decreases from  $a = 2.83, c = 14.87 \text{ \AA}$  to  $a = 2.89, c = 14.48 \text{ \AA}$ . This observation renders  $R = 2.89 \text{ \AA} \lesssim R_c$ .

Based on the idea that  $\text{V}_3$  trimers are formed below  $T_i$  in  $\text{LiVO}_2$  because of an  $R \leq R_c$  and the observation of localized  $\text{V}^{3+}$ -ion moments ( $R > R_c$ ) in the normal spinel  $\text{Mn}[\text{V}_2]\text{O}_4$ , it was thought possible to determine experimentally the room-temperature value of  $R_c$  in the vanadium oxides for an array of octahedral-site  $\text{V}^{3+}$  ions sharing octahedral-site edges with  $z = 6$  nearest like neighbors.<sup>11</sup> In such a determination, it is necessary to distinguish oxides containing vanadium atoms with a single-valence state from those with vanadium in a mixed-valence state as occurs, for example, in  $\text{Li}[\text{V}_2]\text{O}_4$ .

Conceptually, as  $R$  decreases to  $R_c$  in a single-valent system, the bandwidth  $W$  increases and the on-site correlation energy  $U$  decreases toward crossover where the compound changes from a magnetic semiconductor with  $R > R_c$  and  $W < U$  to a metal with  $R < R_c$  and  $W > U$ .<sup>12</sup> Increased screening of the on-site  $3d$ -electron interactions with decreasing  $R$  creates a rapid change in  $U$  with  $R$

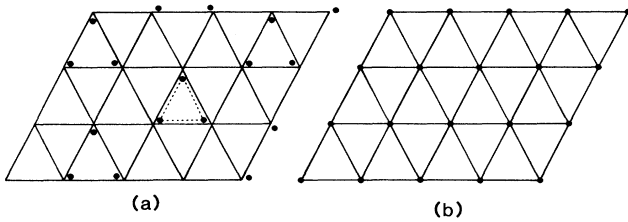


FIG. 1. Proposed arrangement of atoms in vanadium planes of  $\text{LiVO}_2$  (a) below  $T_t$  and (b) above  $T_t$ , showing  $\text{V}_3$  clustering below  $T_t$ .

near  $R \approx R_c$ , which may cause the change from  $R > R_c$  to  $R < R_c$  to be discontinuous via a first-order phase change. A demonstration of the character of the changeover would be instructive.

An initial attempt to determine an  $R_c$  experimentally involved a study of the normal spinels  $A^{2+}[\text{V}_2]\text{O}_4$ , where  $A = \text{Mg, Mn, Fe, Co, and Zn}$ .<sup>11</sup> In these normal spinels, an array of octahedral-site  $\text{V}^{3+}$  ions shares common edges with  $z = 6$  nearest neighbors as in  $\text{LiVO}_2$ . However, the layered oxide  $\text{LiVO}_2$  has a degree of freedom—namely, the variation of the  $c/a$  ratio—that is not available to the cubic spinels where the  $[\text{V}_2]\text{O}_4$  framework is three dimensional. All the spinels contained localized V  $3d$  electrons, so the study only gave an upper limit of 2.97 Å for  $R_c$ , the V-V separation in  $\text{Co}[\text{V}_2]\text{O}_4$ .

Following the observation<sup>13</sup> that Li can be inserted at room temperature into the spinel structure  $A[\text{B}_2]\text{O}_4$  without perturbing the  $[\text{B}_2]\text{O}_4$  framework, the ordered rocksalt  $\text{Li}_2[\text{V}_2]\text{O}_4$  was prepared<sup>8,14,15</sup> by room-temperature Li insertion into the mixed-valent spinel  $\text{Li}[\text{V}_2]\text{O}_4$ . This “soft-chemistry” procedure allowed preparation of a single-valent spinel framework  $[\text{V}_2^{3+}]\text{O}_4$  with a V-V separation  $R = 2.93$  Å. However,  $\text{Li}_2[\text{V}_2]\text{O}_4$  is an antiferromagnetic semiconductor, which renders  $R_c < 2.93$  Å. In view of the evidence for  $\text{V}_3$  trimer formation in  $\text{LiVO}_2$ , which has a V-V separation at  $T_t$  of 2.89 Å, it was concluded<sup>8,15</sup> that the critical V-V separation is restricted to the narrow range

$$2.89 \lesssim R_c < 2.93 \text{ \AA} \quad (3)$$

for oxides containing octahedral-site  $\text{V}^{3+}$  ions sharing common octahedral-site edges with  $z = 6$  nearest neighbors.

On the other hand, Reuter *et al.*<sup>16,17</sup> used infrared spectroscopy to identify a smooth transition from semiconductor to metallic behavior at  $x \approx 0.55$  for  $A_{1-x}\text{Li}_x[\text{V}_2]\text{O}_4$  mixed-valent spinels with  $A = \text{Mg}$  or  $\text{Zn}$ . The V-V separation at this transition led to an apparent  $R_c \approx 2.94$  Å for a  $\text{V}^{4+/3+}$  mixed-valent system. However, the paramagnetic susceptibility of the metallic end member  $\text{Li}[\text{V}_2]\text{O}_4$  obeys a Curie-Weiss law typical of localized magnetic moments on the vanadium atoms but without undergoing magnetic ordering to lowest temperatures.<sup>15,18,19</sup> This observation indicates that the electrons remain strongly correlated in metallic  $\text{Li}[\text{V}_2]\text{O}_4$  and that

the transition identified by Reuter *et al.*<sup>16,17</sup> needs further consideration. Indeed, recent experiments on the system  $\text{Li}_x\text{Zn}_{1-x}[\text{V}_2]\text{O}_4$  reveal a somewhat more complex behavior. First, although the Seebeck data<sup>20</sup> were consistent with a smooth semiconductor-metal transition with increasing  $x$  in the range  $0.3 < x_c < 0.4$ , they could be interpreted in terms of the coexistence of two types of conductive pathways within a single atomic phase: band conduction in one and variable-range hopping in the other. Second, magnetic-susceptibility<sup>21</sup> and neutron-diffraction<sup>22</sup> data indicate antiferromagnetic order at lowest temperatures in  $\text{Zn}[\text{V}_2]\text{O}_4$  with a  $\text{V}^{3+}$ -ion atomic moment  $\mu_v \approx (0.8 \pm 0.4)\mu_B$  and the appearance of a weak ferromagnetic component (phase) on the initial substitution of Li for Zn. Third, the magnetic-susceptibility data<sup>21</sup> also revealed two distinguishable paramagnetic temperature domains,  $T > 500$  K and  $T_N < T < 500$  K, each with distinguishable Curie-Weiss parameters. For  $T > 500$  K the parameters were typical for localized, mixed-valent  $\text{V}^{3+}, \text{V}^{4+}$  configurations; for  $T < 500$  K, the Curie constant  $C$  and Weiss constant  $\Theta$  had larger magnitudes in  $\text{Zn}[\text{V}_2]\text{O}_4$ . Moreover, NMR data in the temperature range  $10 < T < 300$  K (Ref. 7) revealed the presence of two distinguishable electronic pathways (phases) within an atomically single-phase system  $\text{Li}_x\text{Zn}_{1-x}[\text{V}_2]\text{O}_4$ ; a metallic pathway associated with mixed-valent  $\text{V}^{4+}, \text{V}^{3+}$  ions neighboring  $A$ -site  $\text{Li}^+$  ions and a semiconductor pathway associated with single valent regions of  $\text{V}^{3+}$  ions neighboring all  $A$ -site  $\text{Zn}^{2+}$  ions. The semiconductor-metal transition observed in  $\text{Li}_x\text{Zn}_{1-x}[\text{V}_2]\text{O}_4$  at a critical Li concentration  $x_c$  was therefore interpreted to represent a percolation threshold for the metallic pathway (electronic phase). Surprisingly, the NMR data also revealed little electronic crossover between the two phases and a nonmagnetic  $\text{V}^{3+}$ -ion ground state in the semiconductor pathway (electronic phase). A nonmagnetic ground state below 400 K in the semiconductor pathway implies strong antiferromagnetic ordering within cluster fluctuations within the  $[\text{V}_2]\text{O}_4$  spinel framework. The strong spin pairing within cluster fluctuations is apparently broken up by the introduction of  $\text{V}^{4+}$  ions, and this breakup of the cluster fluctuations produces a distinguishable electronic pathway that coexists with the spin-paired pathway.

The picture that emerges from these experiments is the existence of an intrinsic electronic instability associated with an  $R \rightarrow R_c$  that, in a single-valent system, may be manifest as a static charge-density wave (CDW). In a mixed-valent-system, segregation into two distinguishable electronic phases within an atomically single-phase system may also occur. The two electronic phases may be statically separated where there is a mixed array of counter cations; however, it is also possible to envisage a dynamic segregation via charge-density fluctuations (CDF's) as has been postulated<sup>1</sup> to occur in the high- $T_c$  copper oxide superconductors.

### B. Pinpointing $R_c$

To narrow further the range (3) for  $R_c$ , we have returned to  $\text{LiVO}_2$  and inquired at what concentration  $y$  of

Cr in  $\text{LiV}_{1-y}\text{Cr}_y\text{O}_2$  a transition occurs from  $R < R_c$  to  $R > R_c$ . Figure 2 shows the variation with  $y$  of the lattice parameters,  $c/a$  ratio, and the cell volume at room temperature and at  $250^\circ > T_i$ . In the compositional range  $0 \leq y \leq 0.25$ , the substitution of a smaller ( $r_{\text{Cr}} = 0.615 \text{ \AA}$ )  $\text{Cr}^{3+}$  ion for a  $\text{V}^{3+}$  ion ( $r_{\text{V}} = 0.64 \text{ \AA}$ ) causes an anomalous increase with  $y$  in the room-temperature  $a$  parameter and volume; at  $T \approx 250^\circ\text{C} > T_i$  these parameters decrease as expected, but more rapidly than in the interval  $0.3 < y < 1.0$ . Note that the strong temperature dependence of the parameters in the region  $0 < y \leq 0.25$  is due to the traversal of  $T_i$  between room temperature and  $250^\circ\text{C}$ .

The discontinuity in the variations with  $y$  of lattice parameters and cell volume at  $y \approx 0.25$  suggests that the compositions with  $0 \leq y \leq 0.25$  belong to a phase electronically distinguishable from the one for compositions with  $0.3 \leq y \leq 1.0$ . This conclusion is supported by the fact that, although samples with  $0 \leq y \leq 0.25$  and

$0.35 \leq y \leq 1.0$  could be made easily, the  $y = 0.3$  sample was difficult to obtain as a single-phase material.

An octahedral-site  $\text{Cr}^{3+}$  ion carries a localized  ${}^4A_{2g}$   $3d$ -electron configuration  $a_1^1 e_\pi^2 e_\sigma^0$ , where the two  $e_\sigma$  orbitals are  $\sigma$  bonding whereas the  $a_1$  and  $e_\pi$  orbitals have  $t_2$ -orbital parentage in the absence of a trigonal component to the crystalline field. The  $e_\pi$ - $e_\sigma$  hybridization increases with the strength of the trigonal component of the crystalline field. In  $\text{LiCrO}_2$  these localized configurations can be expected to impart a  $\text{Cr}^{3+}$ -ion magnetic moment of approximately  $3\mu_B$  with antiferromagnetic Cr-Cr superexchange interactions within a plane; there is no clustering into  $\text{Cr}_3$  trimers and the condition  $R > R_c$  is applicable in  $\text{LiCrO}_2$ . In the system  $\text{LiV}_{1-y}\text{Cr}_y\text{O}_2$ , the  $\text{Cr}^{3+}$  ions retain their localized configurations, and the condition  $R > R_c$  holds for the Cr-V interactions. Reduction of the mean number  $\bar{z}$  of near-neighbor V-V interactions at a  $\text{V}^{3+}$  ion reduces the tight-binding bandwidth  $W \approx 2\bar{z}b$ , where  $b$  is given by Eq. (2). As a result,  $R_c$  decreases with increasing  $y$  more rapidly than does the V-V separation  $R$  at  $T > T_i$ ; this decrease can be expected to be enhanced by any induced localization of the V  $3d$  electrons at  $\text{V}^{3+}$  ions neighboring a  $\text{Cr}^{3+}$  ion. Consequently, the critical V-V separation  $R_c$  must be traversed with increasing  $y$  at some critical composition  $y = y_c$ . Therefore we conclude that the phase transition that occurs on crossing the compositional range

$$0.25 \leq y_c \leq 0.3 \quad (4)$$

represents a transition from  $R < R_c$  to  $R > R_c$  at the  $\text{V}^{3+}$  ion array. The fact that the transition is not smooth, but appears to be separated by a narrow two-phase region, has two important implications:

(i) The localized-electron (strongly correlated) and itinerant electron (weakly correlated) regimes for a single-valent array represent two thermodynamically distinguishable states.

(ii) At  $R \approx R_c$ , which corresponds to a  $W \approx U$ , a single-valent system is intrinsically unstable relative to a disproportionation into phases with  $R < R_c$  and  $R > R_c$ .

The lattice-parameter variations with  $y$  for  $y > y_c$  appear to obey a normal Vegard's law. Extrapolation of the room-temperature  $a$  parameter to  $y = 0$  from the localized-electron domain  $0.3 < y \leq 1.0$  gives an upper limit for  $R_c$  of  $2.905 \text{ \AA}$ . Given a lower limit of  $2.89 \text{ \AA}$  in  $\text{LiVO}_2$  itself, we believe the data demonstrate a critical separation distance

$$R_c = 2.90 \pm 0.01 \text{ \AA} \quad (5)$$

The volume dilatation predicted to occur on passing from an  $R < R_c$  to an  $R > R_c$  (Ref. 12) is present, but somewhat obscured by the crystallographic transformation occurring in the  $y < y_c$  ( $R \gtrsim R_c$ ) phase; a similar discontinuous volume increase has been found to occur in several copper oxide systems on passing from the superconductor to the antiferromagnetic phase.<sup>23,24</sup> The large volume expansion on passing from  $T < T_i$  to  $T > T_i$  reflects the first-order character of that transition; the data suggest that in  $\text{LiVO}_2$  the lattice vibrations just

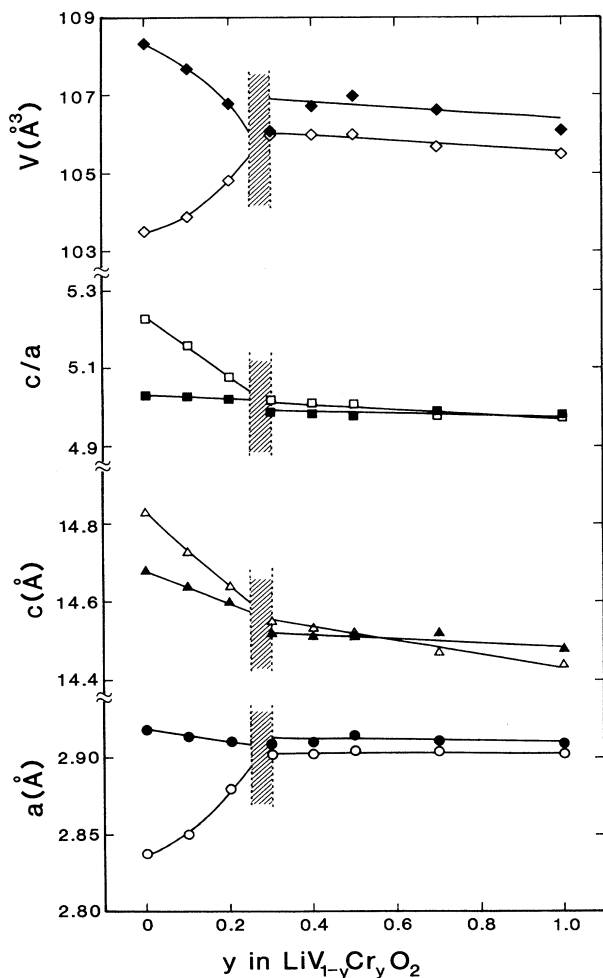


FIG. 2. Variations of lattice parameters and cell volume with  $y$  for  $\text{LiV}_{1-y}\text{Cr}_y\text{O}_2$ ; shaded area indicates a two-phase region. The open and solid symbols refer to the data recorded, respectively, at room temperature and  $250^\circ\text{C}$ .

above  $T_t$  are probably anomalously large at 250°C in anticipation of the structural transformation.

In the itinerant-electron phase ( $0 \leq y < y_c$ ), the remarkable decrease in the  $a$  parameter at room temperature from its value at 250°C reflects not only the anomalous expansion at  $T > T_t$ , but also an added basal-plane V-V bonding at  $T < T_t$ . The localized-electron configurations of the  $\text{Cr}^{3+}$  ions would not share in this basal-plane V-V bonding, so we can anticipate not only an increase in the  $a$  parameter with  $y$  despite the smaller size of a  $\text{Cr}^{3+}$  ion, but also a decrease with increasing  $y$  of both  $T_t$  and of the enthalpy change  $\Delta H$  at  $T_t$ . From the DSC data of Figs. 3 and 4, it is apparent that  $T_t$  falls nearly linearly with increasing  $y$  to about room temperature at  $y \approx 0.2$  whereas  $\Delta H$  drops much more rapidly, falling to about a tenth of its magnitude in  $\text{LiVO}_2$  at  $y \approx 0.2$ . In fact, although the lattice-parameter variation with  $y$  indicates a  $T_t > 280$  K for  $y = 0.2$ , we were unable to detect with DSC a phase transition in any sample with  $y \geq 0.2$  down to 77 K. The enthalpy  $\Delta H$  measures the difference between the change in electronic energy that drives the first-order transition and the elastic-energy change that inhibits it; the transition temperature  $T_t$  appears to be controlled by the change in the lattice energy on passing through the tran-

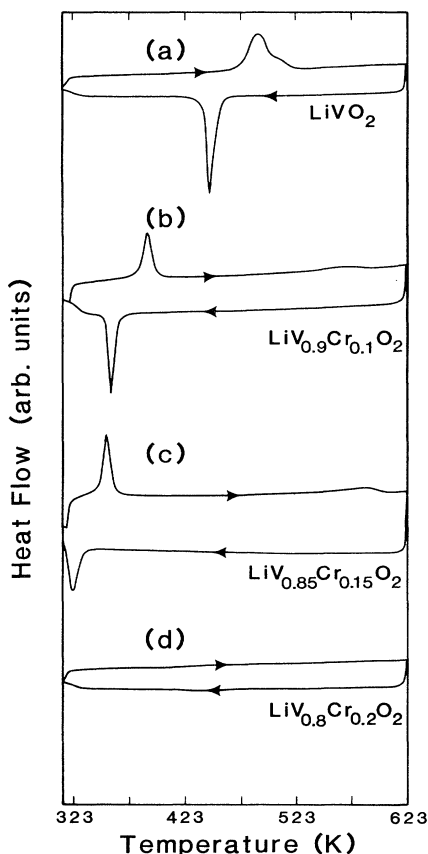


FIG. 3. DSC plots recorded on heating and cooling in  $\text{N}_2$  atm at  $10^\circ\text{C min}^{-1}$  for (a)  $y=0.0$ , (b)  $y=0.1$ , (c)  $y=0.15$ , and (d)  $y=0.2$  in  $\text{LiV}_{1-y}\text{Cr}_y\text{O}_2$ .

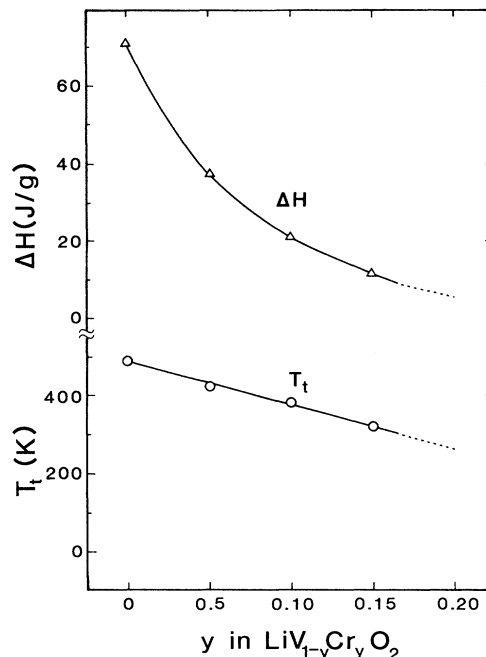


FIG. 4. Variations of enthalpy change  $\Delta H$  and transition temperature  $T_t$  with  $y$  for  $\text{LiV}_{1-y}\text{Cr}_y\text{O}_2$  in the phase  $0 \leq y < 0.25$ .

sition. Consequently  $T_t$  remains finite throughout the compositional range  $0 \leq y < y_c$ , disappearing discontinuously on entering the localized-electron phase  $y_c < y \leq 1.0$ . On the other hand,  $\Delta H$  drops to a small value within the compositional range  $0 \leq y < y_c$ .

Finally, the formation of cation clusters with  $R < R_c$  within a cluster (molecular orbitals) and  $R > R_c$  between clusters may be considered an internal disproportionation into  $R < R_c$  and  $R > R_c$  distances via atomic displacements rather than by atomic diffusion. In this sense, formation of  $\text{V}_3$  trimers is an expression of the intrinsic instability associated with a phase having  $R \approx R_c$ , i.e.,  $W \approx U$ .

### C. The system $\text{LiV}_{1-y}\text{Ti}_y\text{O}_2$

Unlike  $\text{Cr}_2\text{O}_3$ , which is an antiferromagnetic insulator,  $\text{Ti}_2\text{O}_3$  contains itinerant  $3d$  electrons and exhibits a smooth semiconductor-metal transition associated with a band-edge crossing on raising the temperature.<sup>25</sup> Therefore, a  $\text{Ti}^{3+}$  ion might participate with  $\text{V}^{3+}$  ions in the formation of cation clusters. However, with only one  $3d$  electron per  $\text{Ti}^{3+}$  ion, any triangular clusters containing  $\text{Ti}^{3+}$  ions would be electron deficient. Moreover, the difference in electronic potentials at the  $\text{Ti}^{3+}$  and  $\text{V}^{3+}$  ions makes less stable the participation of a  $\text{Ti}^{3+}$  ion in molecular-orbital formation with  $\text{V}^{3+}$  ions; stronger Ti-Ti interactions could become competitive. Therefore  $\Delta H$  and  $T_t$  can be expected to decrease with  $y$  in  $\text{LiV}_{1-y}\text{Ti}_y\text{O}_2$  also, but somewhat less steeply than occurs in  $\text{LiV}_{1-y}\text{Cr}_y\text{O}_2$ , and strong Ti-Ti interactions could lim-

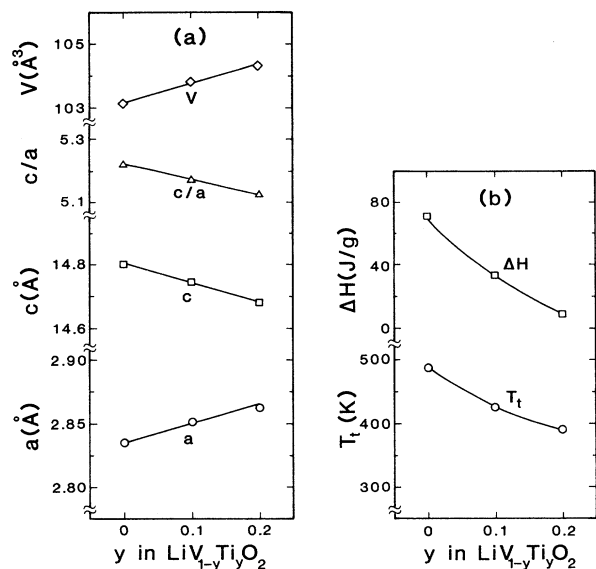


FIG. 5. Variations of (a) lattice parameters and cell volume and (b) enthalpy change  $\Delta H$  and transition temperature  $T_t$  with  $y$  for  $\text{LiV}_{1-y}\text{Ti}_y\text{O}_2$ .

it the range of solid solubility.

Indeed, x-ray powder diffraction revealed that the solid solution of Ti in  $\text{LiV}_{1-y}\text{Ti}_y\text{O}_2$  is limited to the range  $0 \leq y \leq 0.2 < y_c$ . The variation with  $y$  of the room-temperature ( $T < T_t$ ) lattice parameters and cell volume is shown in Fig. 5(a); the variation of  $T_t$  and  $\Delta H$  with  $y$  is shown in Fig. 5(b). In this system also, the drop in  $\Delta H$  with increasing  $y$  is much more precipitous than the drop in  $T_t$ , but neither of these variables drops as steeply with  $y$  as they do in  $\text{LiV}_{1-y}\text{Cr}_y\text{O}_2$ .

Although no direct information on the value of  $R_c$  is forthcoming from this system, the data are consistent with an instability for  $R \approx R_c$  that extends in this system to  $y=1$ ; even the end member  $\text{LiTiO}_2$  is reported to be contaminated with other phases such as  $\text{Li}_2\text{TiO}_3$ .<sup>26</sup>

#### IV. THE SYSTEM $\text{LiVO}_2$ - $\text{VO}_2$

DSC plots for the system  $\text{Li}_{1-x}\text{VO}_2$  are shown in Fig. 6; the different compositions were obtained by extracting Li from  $\text{LiVO}_2$  at room temperature with a  $\text{Br}_2$  solution. As observed previously,<sup>8</sup> the  $T_t$  obtained in the first heating cycle increases from 490 K at  $x=0$  to 550 K at  $x=0.125$ , but it remains constant for all  $x$  in the interval  $0.125 \leq x \leq 0.33$  although  $\Delta H$ , Fig. 7, decreases monotonically with  $x$  throughout the range  $0 \leq x \leq 0.33$ . The disproportionation reaction (1) above  $T_t$  into  $\text{LiVO}_2$  and  $\text{Li}[\text{V}_2]\text{O}_4$  returns the observed  $T_t$  to 490 K on cooling and on the second heating cycle for all  $x$ ; the phase  $\text{Li}[\text{V}_2]\text{O}_4$  contributes no signal. Of particular interest for this study is the behavior below  $T_t$  in the range  $0 < x < 0.125$ , which has not previously been explored.

On heating, the DSC curves exhibit two peaks in the range  $0 < x < 0.125$ , which indicates the presence of two

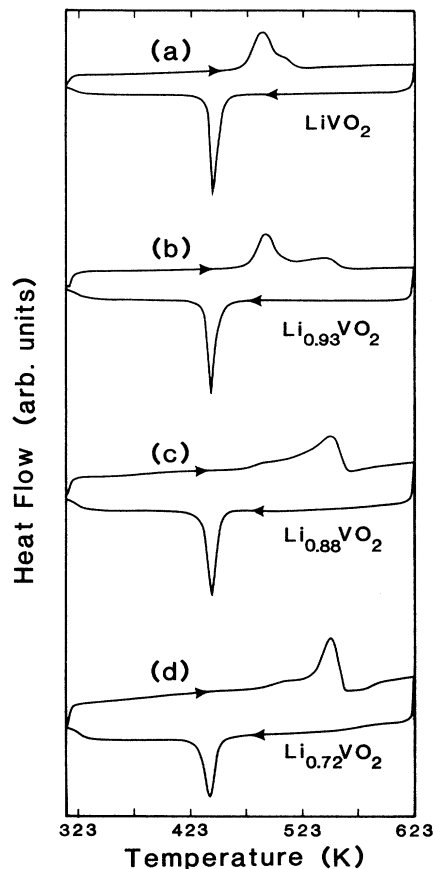


FIG. 6. DSC plots recorded on heating and cooling in  $\text{N}_2$  atm at  $10^\circ\text{C min}^{-1}$  for (a)  $x=0.0$ , (b)  $x=0.07$ , (c)  $x=0.12$ , and (d)  $x=0.28$  in  $\text{Li}_{1-x}\text{VO}_2$ .

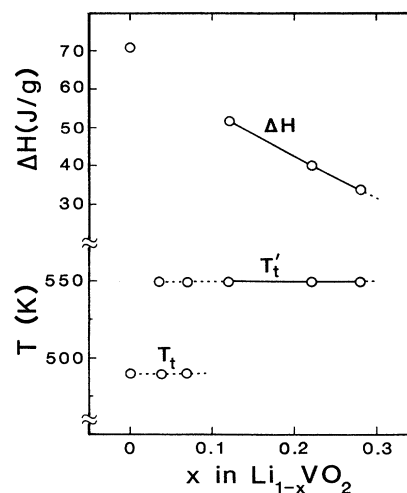


FIG. 7. Variations of enthalpy change  $\Delta H$  and transition temperatures  $T_t$  or  $T'_t$  with  $x$  for  $\text{Li}_{1-x}\text{VO}_2$ . In the two-phase region  $0 < x < 0.12$ , the  $\Delta H$  values are not shown.

distinguishable low-temperature phases each with its own value of  $T_t$ . We designate them  $T_t \approx 490$  K for  $\text{LiVO}_2$  and  $T_t' \approx 550$  K for  $0.12 < x \leq 0.33$ .

An increase in  $T_t$  with decreasing electron concentration in the clusters would seem to be inconsistent with the stabilization of  $\text{V}_3$  trimers below  $T_t$  in  $\text{LiVO}_2$ . Therefore, it was postulated<sup>8</sup> that this anomaly probably reflects the introduction of a ferroelectric-type displacement of  $\text{V}^{4+}$  ions away from each other across a broken bond in a trimer deficient in two electrons. Such a model requires the capture of two holes per electron-deficient trimer at two vanadyl units  $(\text{VO})^{2+}$  in  $\text{V}(\text{VO}_2)$  clusters coexisting with  $\text{V}_3$  trimers. In order to test this speculation, room-temperature infrared data for  $\text{Li}_{0.7}\text{VO}_2$  and  $\text{VO}_2$  were taken and compared. It is known that the transition below  $67^\circ\text{C}$  in  $\text{VO}_2$  involves not only the formation of dimers, but also the rocking of the dimers to form vanadyl  $(\text{VO})^{2+}$  species.<sup>12,27</sup> In  $\text{VO}_2$ , an infrared peak appears near  $980\text{ cm}^{-1}$ , the position for the vanadyl ion<sup>28</sup>; in  $\text{Li}_{0.7}\text{VO}_2$  this peak is absent. Therefore, we seem forced to conclude that there is no vanadyl formation in the oxidized  $\text{VO}_2$  planes of  $\text{Li}_{1-x}\text{VO}_2$ ,  $0.12 < x \leq 0.33$ . This conclusion is also consistent with a monotonic decrease in  $\Delta H$  with  $x$ . Thus, these results reinforce the deduction that the transition temperature  $T_t$  is controlled more by the lattice-energy change through the distortion than by the  $\Delta H$  of the transition; indeed, the low-temperature phases for  $\text{LiVO}_2$  and  $\text{Li}_{1-x}\text{VO}_2$  with  $0.12 < x \leq 0.33$  must be structurally distinguishable since they represent distinguishable phases.

These studies, together with the detailed investigation of the  $\text{Li}_{1-x}\text{VO}_2$  and  $\text{Li}_{1+x}\text{V}_2\text{O}_4$  systems reported previously,<sup>8</sup> yield the phase diagrams of Figs. 8 and 9 for the system  $\text{LiVO}_2$ - $\text{VO}_2$ .  $\text{LiVO}_2$  is a line phase—limited solubility range not determined—that is stable to at least  $750^\circ\text{C}$ . It undergoes a structural transformation at  $T_t \approx 490$  K. The spinel phase  $\text{Li}[\text{V}_2]\text{O}_4$  may also be obtained by high-temperature synthesis,<sup>29</sup> but more easily

by room-temperature extraction of half of the Li from  $\text{LiVO}_2$  followed by heating to above  $550$  K.<sup>8</sup> The spinel phase undergoes no structural transformation to lowest temperatures. The end member  $\text{VO}_2$  is also accessible by high-temperature synthesis; it undergoes a structural transformation at  $67^\circ\text{C}$ .<sup>30</sup> This relatively simple phase diagram is given in Fig. 8.

Two distinct metastable phase diagrams may be obtained below  $550$  K; Fig. 9 is relevant under conditions where Li is extracted from  $\text{LiVO}_2$ ; another (not shown) can be obtained by Li insertion/extraction into/from the spinel  $\text{Li}[\text{V}_2]\text{O}_4$ . Figure 9 shows a metastable phase in the compositional range  $0.12 < x \leq 0.33$  that disproportionates above  $T_t' = 550$  K into  $\text{LiVO}_2$  and  $\text{Li}[\text{V}_2]\text{O}_4$ . Two-phase regions exist for  $0 < x \leq 0.12$  and  $0.33 < x < 0.67$ . The phase  $\text{Li}_{0.33-x}\text{VO}_2$  is stabilized by an ordered arrangement of one-third of the V atoms in the planes that were originally all Li atoms.<sup>31</sup> Room-temperature electrochemical extraction of Li from  $\text{LiVO}_2$  (Ref. 32) indicates the presence of phases over the range  $0.33 < x < 0.67$  whereas the domain  $0.125 \leq x \leq 0.33$  shows an open-circuit voltage  $V_{oc}$  varying smoothly with  $x$  as for a solid-solution range. Like  $\Delta H$ , the open-circuit voltage tracks the total number of electrons active in V-V bonding whereas  $T_t$  reflects some other parameter—presumably the change in lattice energy through the structural transformation.

The metastable phase diagram obtained from Li insertion into  $\text{Li}[\text{V}_2]\text{O}_4$  is much simpler; it yields the solid-solution range  $\text{Li}_{1+x}[\text{V}_2]\text{O}_4$ ,  $0 \leq x \leq 1$ , in which the  $[\text{V}_2]\text{O}_4$  spinel framework stays intact and the  $\text{Li}^+$  ions occupy an increasing proportion of octahedral sites with increasing  $x$  until, at  $x = 1$ , the ordered rocksalt phase  $\text{Li}_2[\text{V}_2]\text{O}_4$  is obtained. What happens on extraction of Li from  $\text{Li}[\text{V}_2]\text{O}_4$  has not been studied carefully. It appears that there is no large solid-solution range between  $\text{Li}[\text{V}_2]\text{O}_4$  and cubic  $[\text{V}_2]\text{O}_4$ —as occurs, for example, in the system  $\text{Li}_{1-x}[\text{Mn}_2]\text{O}_4$ , but rather a conversion to the

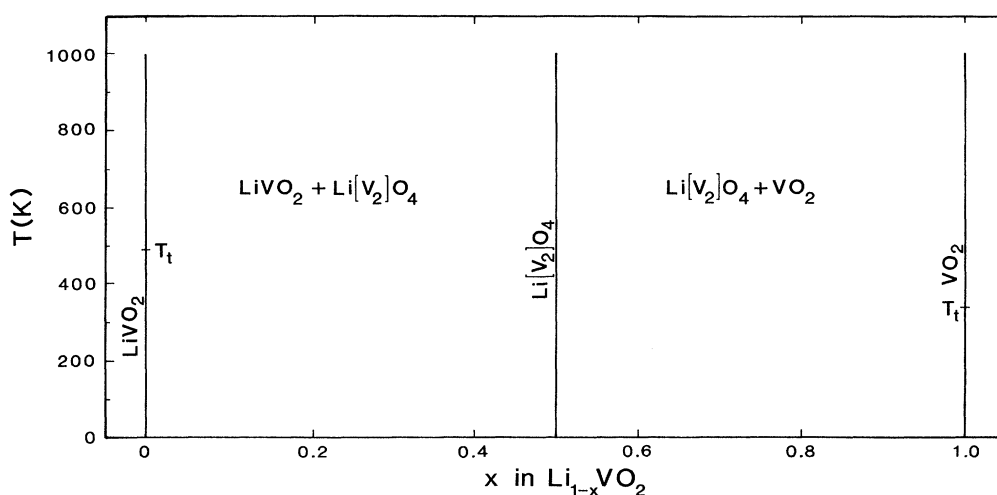


FIG. 8. Equilibrium phase diagram for the system  $\text{LiVO}_2$ - $\text{VO}_2$  prepared above  $550$  K.

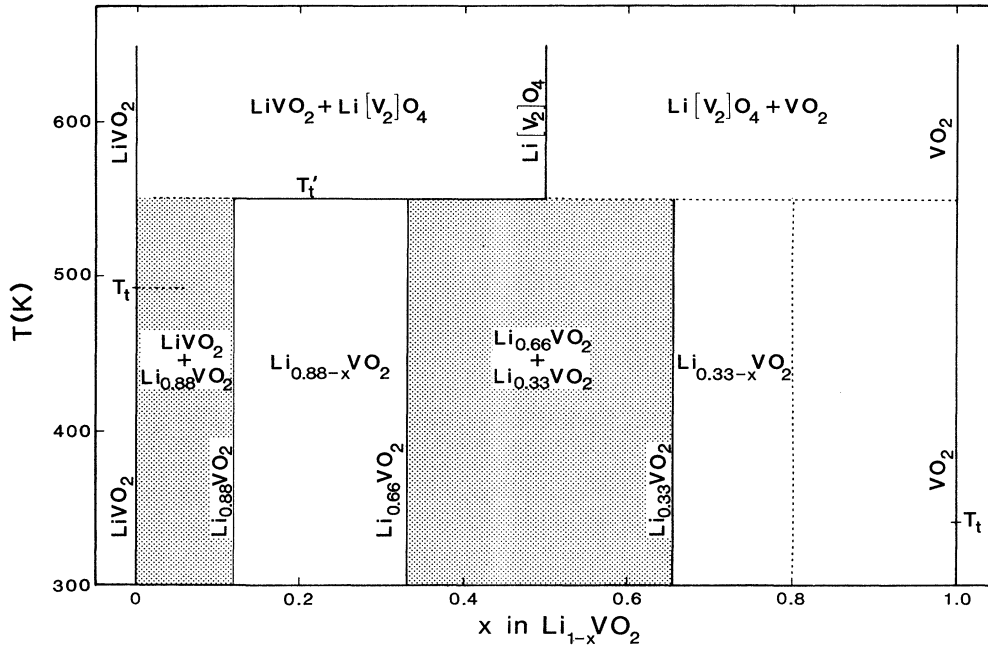


FIG. 9. Phase diagram for the system  $\text{LiVO}_2\text{-VO}_2$  obtained on heating samples prepared by room-temperature extraction of Li from  $\text{LiVO}_2$ .

layered phase  $\text{Li}_{0.33}\text{V}_2\text{O}_4$ . It may prove significant that  $2.93 > R > 2.91 \approx R_c$  in the range  $\text{Li}_2[\text{V}_2]\text{O}_4$  to  $\text{Li}[\text{V}_2]\text{O}_4$ . Extraction of Li in  $\text{Li}_{1-x}[\text{V}_2]\text{O}_4$  forces the condition  $R \approx R_c$ , which we predict to be unstable.

### V. CONCLUSIONS

We have demonstrated that  $R_c \approx 2.90 \pm 0.01 \text{ \AA}$  for the room-temperature V-V separation in an oxide with an array of  $\text{V}^{3+}$  ions sharing common octahedral-site edges with  $z = 6$  like near neighbors. We have shown that the condition  $R \approx R_c$ , which corresponds to a  $W \approx U$ , is intrinsically unstable. In the single-valent system  $\text{LiV}_{1-y}\text{Cr}_y\text{O}_2$ , for example, this instability is manifest in a two-phase compositional range separating  $R < R_c$  for  $y < y_c$  from  $R > R_c$  for  $y > y_c$ . In the system  $\text{Li}_{1-x}\text{VO}_2$ , the single-valent end member ( $x = 0$ ) forms  $\text{V}_3$  trimers below  $T_t \approx 490 \text{ K}$ , and a two-phase region in the interval  $0 < x \leq 0.12$  separates the single-valent phase from the mixed-valent compositional range. Moreover, the mixed-valent compositions disproportionate above  $T'_t = 550 \text{ K}$  into  $\text{LiVO}_2$  and the spinel  $\text{Li}[\text{V}_2]\text{O}_4$ . We have also shown that the transition temperature  $T_t$  below which a CDW is formed is controlled more by the lattice-energy change associated with the structural transformation than by the total enthalpy change  $\Delta H$  associated with the transition.

Metastable phase diagrams below  $550 \text{ K}$  have been obtained for the  $\text{LiVO}_2\text{-VO}_2$  system by room-temperature Li extraction from  $\text{LiVO}_2$  and by Li insertion or extraction into or from  $\text{Li}[\text{V}_2]\text{O}_4$ .

Comparisons have been made between the high- $T_c$  copper oxides and the vanadium oxides. In the superconductor copper oxides, the condition  $W \approx U$  is also encountered; a large on-site  $U$  inhibits the formation of a negative- $U$  CDW, as is also the case in the vanadium oxides discussed. The bandwidth  $W$  in the copper oxides is associated with nearly  $180^\circ$  Cu-O-Cu interactions; it is sensitive to the hole concentration in an oxidized  $\text{CuO}_2$  layer because the covalent-mixing parameter  $\lambda_\sigma$  reflects a system near crossover from a more ionic to a more covalent Cu: $3d\text{-O}:2p_\sigma$  bonding.<sup>33</sup> The bandwidth  $W$  in the vanadium oxides discussed is associated with V-V interactions that vary exponentially with the V-V separation  $R$  across shared octahedral-site edges. In both the copper oxides and the vanadium oxides, intrinsic lattice instabilities appear to be associated with the condition  $W \approx U$ . These instabilities are manifest as static phase segregations, static charge-density waves, and—it would appear—also as dynamic charge-density fluctuations. Where the dynamic charge-density fluctuations give rise to superconductivity and where they give rise to some other phenomenon represents an open and fascinating field of investigation.

### ACKNOWLEDGMENTS

We gratefully acknowledge support for this research by the Robert A. Welch Foundation, Houston, Texas, the National Science Foundation, and the Texas Advanced Research Program.



- <sup>1</sup>J. B. Goodenough and J.-S. Zhou, *Phys. B.* **42**, 4276 (1986).
- <sup>2</sup>R. S. Markiewicz, *Superconductivity and its Application (Buffalo, 1990)*, Proceedings of the Fourth Annual Conference on Superconductivity and its Application, AIP Conf. Proc. No. 219, edited by Yi-Han Kao, Philip Coppens, and Hoi-Sing Kwok (AIP, New York, 1991).
- <sup>3</sup>P. F. Bongers, Ph.D. dissertation, University of Leiden, Leiden, The Netherlands, 1957.
- <sup>4</sup>J. B. Goodenough, *Magnetism and the Chemical Bond* (Interscience and Wiley, New York, 1963), p. 269.
- <sup>5</sup>P. F. Bongers, in *Crystal Structure and Chemical Bonding in Inorganic Chemistry*, edited by C. J. M. Rooymans and A. Rabenau (Elsevier, New York, 1975), Chap. 4.
- <sup>6</sup>F. Takagi, K. Kawakami, I. Maekawa, Y. Sakai, and N. Tsuda, *J. Phys. Soc. Jpn.* **56**, 444 (1987).
- <sup>7</sup>Y. Amako, T. Naka, M. Onoda, H. Nagasawa, and T. Erata, *J. Phys. Soc. Jpn.* **59**, 2241 (1990).
- <sup>8</sup>A. Manthiram and J. B. Goodenough, *Can. J. Phys.* **65**, 1309 (1987).
- <sup>9</sup>K. Vidyasagar and J. Gopalakrishnan, *J. Solid State Chem.* **42**, 217 (1982).
- <sup>10</sup>T. A. Hewston and B. L. Chamberland, *J. Solid State Chem.* **65**, 100 (1986).
- <sup>11</sup>D. B. Rogers, R. J. Arnott, A. Wold, and J. B. Goodenough, *J. Phys. Chem. Solids* **24**, 347 (1963).
- <sup>12</sup>J. B. Goodenough, *Prog. Solid State Chem.* **5**, 145 (1971).
- <sup>13</sup>M. M. Thackeray, W. I. F. David, and J. B. Goodenough, *Mater. Res. Bull.* **17**, 785 (1982); M. M. Thackeray, W. I. F. David, P. G. Bruce, and J. B. Goodenough, *ibid.* **18**, 461 (1983).
- <sup>14</sup>L. A. de Picciotto and M. M. Thackeray, *Mater. Res. Bull.* **20**, 1409 (1985).
- <sup>15</sup>J. B. Goodenough, A. Manthiram, A. C. W. P. James, and P. Strobel, in *Solid State Ionics*, edited by F. Nagri, R. A. Muggins, and D. F. Shriver, MRS Symposia Proceedings No. 135 (Materials Research Society, Pittsburgh, PA, 1989), p. 391.
- <sup>16</sup>B. Reuter and J. Jaskowsky, *Ber. Bunsten-Ges. Phys. Chem.* **70**, 189 (1966).
- <sup>17</sup>B. Reuter and K. Müller, *Naturwissenschaften* **54**, 164 (1967).
- <sup>18</sup>H. Kessler and M. Sienko, *J. Chem. Phys.* **55**, 5414 (1971).
- <sup>19</sup>B. L. Chamberland and T. A. Hewston, *Solid State Commun.* **58**, 693 (1986).
- <sup>20</sup>K. Kawakami, Y. Sakai, and N. Tsuda, *J. Phys. Soc. Jpn.* **5**, 3174 (1986).
- <sup>21</sup>Muhtar, F. Takagi, K. Kawakami, and N. Tsuda, *J. Phys. Soc. Jpn.* **57**, 3119 (1988).
- <sup>22</sup>S. Niziol, *Phys. Status Solidi A* **18**, K11 (1973).
- <sup>23</sup>J. B. Goodenough and A. Manthiram, *Physica C* **157**, 439 (1989).
- <sup>24</sup>A. Manthiram, X. X. Tang, and J. B. Goodenough, *Phys. Rev. B* **42**, 138 (1990).
- <sup>25</sup>L. L. Van Zandt, J. M. Honig, and J. B. Goodenough, *J. Appl. Phys.* **39**, 594 (1968).
- <sup>26</sup>T. A. Hewston and B. L. Chamberland, *J. Solid State Chem.* **59**, 168 (1985).
- <sup>27</sup>R. Heckingbottom and J. W. Linnet, *Nature* **194**, 678 (1962).
- <sup>28</sup>G. Ladwig, *Z. Anorg. Allgem. Chem.* **364**, 234 (1969).
- <sup>29</sup>D. B. Rogers, J. B. Goodenough, and A. Wold, *J. Appl. Phys.* **35**, 1069 (1964); D. B. Rogers, J. L. Gillson, and I. E. Gier, *Solid State Commun.* **5**, 263 (1967).
- <sup>30</sup>G. Andersson, *Acta Chem. Scand.* **10**, 623 (1956).
- <sup>31</sup>M. M. Thackeray, L. A. de Picciotto, W. I. F. David, P. G. Bruce, and J. B. Goodenough, *J. Solid State Chem.* **67**, 285 (1987).
- <sup>32</sup>L. A. de Picciotto, M. M. Thackeray, W. I. F. David, P. G. Bruce, and J. B. Goodenough, *Mater. Res. Bull.* **19**, 1497 (1984).
- <sup>33</sup>J.-S. Zhou, J. B. Goodenough, K. Allan, and A. Champion (unpublished).